symmetry

MDPI

Article

Photo-Thermoelasticity Heat Transfer Modeling with Fractional Differential Actuators for Stimulated Nano-Semiconductor Media

Sameh Askar [1], Ahmed E. Abouelregal [2,*], Marin Marin [3,*] and Abdelaziz Foul [1]

[1] Department of Statistics and Operations Research, College of Science, King Saud University, P.O. Box 2455, Riyadh 11451, Saudi Arabia
[2] Department of Mathematics, Faculty of Science, Mansoura University, Mansoura 35516, Egypt
[3] Department of Mathematics and Computer Science, Transilvania University of Brasov, 500036 Brasov, Romania
* Correspondence: ahabogal@mans.edu.eg (A.E.A.); m.marin@unitbv.ro (M.M.)

Abstract: The term "optical thermoelasticity" is used to describe how the optical properties of a material change when it is heated or deformed mechanically. The issues of effective elastic and heat transfer symmetry are given particular focus. This study gives a new nonlocal theoretical formulation for a thermo-optical elastic material that can be used to describe how thermomechanical waves and plasma waves relate to the symmetry of semiconductor materials such as silicon or germanium. The suggested model includes the idea of nonlocal elasticity and a modified Moore–Gibson–Thompson (MGT) heat conduction equation with nonsingular fractional derivative operators. The heat transfer equation has been converted and generalized into a nonsingular fractional form based on the concepts of Atangana and Baleanu (AB) using the Mittag–Leffler kernel. The developed model is used to examine the effect of thermal loading by ramp-type heating on a free plane of unbounded semiconductor material symmetries. Using the Laplace transform approach, we may analytically obtain linear solutions for the investigated thermo-photo-elastic fields, such as temperature. The Discussion section includes a set of graphs that were generated using Mathematica to evaluate the impact of the essential parameters.

Keywords: nonlocal thermoelasticity; photo-excitation; ramp-type; fractional Atangana and Baleanu operator

MSC: 35Q79; 35B40; 35J55; 73B30; 45F15

Citation: Askar, S.; Abouelregal, A.E.; Marin, M.; Foul, A. Photo-Thermoelasticity Heat Transfer Modeling with Fractional Differential Actuators for Stimulated Nano-Semiconductor Media. *Symmetry* **2023**, *15*, 656. https://doi.org/10.3390/sym15030656

Academic Editor: Juan Luis García Guirao

Received: 16 January 2023
Revised: 17 February 2023
Accepted: 4 March 2023
Published: 6 March 2023

1. Introduction

There has been a new rise of interest in the photoacoustic (PA) impact as the fundamental physics behind a variety of techniques for studying the optical properties, heat transfer, and mechanical and electrical properties of condensed media, particularly semiconducting material symmetry. The symmetries of flexible semiconductor materials are referred to as physical symmetries. It finds widespread application in detecting defects and larger tolerances in opaque objects. In a similar vein, physical studies of the effect of PA have advanced significantly [1]. In the field of continuum mechanics, symmetry is important because it can show how materials behave and the properties of solutions to boundary-value problems that are important. The absorption of photons of various intensities by materials and their subsequent conversion into heat is the ubiquitous and fundamental mechanism upon which the PA influence is based. The crackling and popping sounds caused by thermal expansion are one of the techniques used to identify the resultant heat waves. Taking into account fluctuations in measured temperatures can shed light on the thermal characteristics of a material with uniform symmetry, the nature of its flaws and heterogeneities, and the conditions under which heat waves travel. As a result, heat sources offer information on the photon-to-thermal energy conversion process, including

the absorption coefficient, the movement of absorbed energy, and the presence or absence of heterogeneity [2,3].

Since heat waves have a critical role in the PA influence and associated phenomena, the term "PA influence" has recently been replaced by the term "photothermal influence," which is well suited if non-thermal sound sources are not present. Due to the inclusion of non-thermal forcing processes for PA, the thermoelastic interaction of a material with radiation must be determined by more than just the displacement field [4]. Non-constant temperature (mostly on the surface of an object) and deformation measurements are often used to probe the influence of PA (usually also on the surface of an object). In the present work, responses to changes in temperature and motion within semiconducting media will be studied. Through experimental results, it was observed that mechanical stress appeared in semiconductors and microelectromechanical devices after electron-hole plasma generation. The mechanism of electronic deformation relies on the fact that the photogenerated plasma changes the crystal structure and the effective symmetry of the material, which in turn alters the potential of the conduction and valence bands in the semiconductor. This indicates that photocarriers may induce local stress in the material. Like thermal asymmetry waves, which are generated by local periodic elastic deformation, this strain may alter the propagation of plasma waves in semiconductors [5].

However, Rosenzweig and Gersho's hypothesis suffers from a major flaw that severely limits its applicability, notably in the field of semiconductors. The downside is that the true process of turning light energy into heat is not considered. Absorption of light is known to result in the creation of transient electron excitations that can only travel a limited distance in that period [6]. When electron excitations settle down to their ground states, energy is released as heat. In this case, the spatial and temporal dependencies of the heat source functions are distinct from those of the light intensity. Electron excitations at the surface of semiconducting material symmetry can recombine with the roughness of the potential relief, which generates additional heat. The PA impact in semiconductors is also crucial to study because of the nonthermal sound sources that might result from nonequilibrium charge carrier interplay with the lattice [7].

The term "MEMS" refers to a system that uses microfabrication and nanotechnology to combine mechanical, sensor, actuator, and electrical components onto a single integrated circuit. Microelectromechanical systems (MEMS) comprise both silicon-based and non-silicon-based devices made using micromachining technology initially designed to make integrated circuits. Sensors, actuators, and passive structures are the three broad categories that describe them [8]. Devices that combine electrical and mechanical capabilities at the nanoscale are known as nanoelectromechanical systems (NEMS). Microelectromechanical systems (MEMS) have paved the way for the development of NEMS devices, which are the next logical step in the miniaturization process. Nanoelectromechanical systems (NEMS) often utilize transistor-like nanoelectronics in conjunction with mechanical actuators, pumps, or engines to produce physicochemical sensors [9]. When used as mechanical biosensors during surgery, NEMSs offer three primary benefits. Because the least detectable mass added is directly proportional to the overall mass of the device, they are capable of mass resolution on the nanogram scale even while working in a fluid environment. Second, uniformly decreasing a NEMS device's size enhances its capacity to be shifted or distorted, a property known as mechanical compliance.

Classical continuum mechanics postulates that all materials are composed of an infinite number of points, such as particles that can only move with respect to their nearest neighbors. There are few applications for classical mechanics since it does not specify the material's discrete structure or reveal numerous microscopic processes such as microdeformation and microdislocation. In light of this discovery, it became apparent that a unified perspective was necessary to instill the concept that a material particle is a volume element that would deform and rotate and that the material is generally a multiscale material. Calculating its equilibrium also requires taking into account the particle's nonlocal interactions

with other particles in the medium. Based on these things, the material model can be seen as a nonlocal micro-continuum theory.

As is often known, the laws of conventional continuum mechanics (CCM) do not change with the dimensions of the system being studied. Given the nature of its system of equations, it is unable to forecast any size effect. It may thus fail in situations where such factors as size dependency and scaling of mechanical phenomena play a significant role. All of the aforementioned issues are solvable with discrete models, but doing so is computationally intensive. Because of this, there has been a push to formulate models of modified continuum mechanics that can account for size effects by including intrinsic lengths.

The modern form of nonlocal mechanics was established by Eringen and colleagues [10–12]. Nonlocal theories describe particles of matter as points of mass that can only translate and not spin or rotate. As the distance between the particles increases, their long-range interactions weaken, and attenuation functions are created to represent this phenomenon. Constitutive equations have been derived from these functions, and the integral functions for kinematic variables define the equilibrium equations in continuum theory. This was similar to the theories of classical mechanics. Nonlocal continuum mechanics on small scales was introduced to be more inclusive of local mechanics [13].

In the field of thermoelasticity, Biot [14] created the coupled heat transfer (CTE) model, which is based on Fourier's law of heat flux transfer rate. This model has been used in many modern technologies, especially those that involve high temperatures. These models do not work well at low temperatures or when there are sudden changes in temperature. The traditional models associated with infinite velocities of thermal signals are also assumed but are not acceptable physically. To address this problem, many ideas and suggestions were presented. Lord and Shulman made one of the most famous of these proposals [15] (LS) by adding an additional term to the heat flux differential and including the concept of relaxation or phase delay in the Fourier equation of heat transfer. In this context, Green and Naghdi [16–18] also proposed three different types of thermal conductivity equations, which are referred to by the abbreviations GN-III, GN-II, and GN-I. The first model GN-I is similar to conventional correlated thermoelasticity. In contrast, the second model, GN-II, shows the rate-limited transmission of thermal signals without energy loss. The last type of Green and Naghdi models, GN-III, shows an unlimited diffusion rate with energy dissipation.

The Moore–Gibson–Thompson (MGT) concept has gained popularity recently because it allows scientists to understand many physical properties of many phenomena in flexible semiconducting materials. Models incorporating the MGT equation are largely concerned with studying the behavior of waves as they travel through media, especially liquid and viscous rubber materials. This rate relies heavily on including relaxation periods (thermal memory) in the transport equations in order to represent the medium under study more accurately [19]. Modifying the system of equations within the context of the Green–Naghdi type III theory, Quintanilla [20,21] developed a new version of the improved thermoelasticity concept that significantly expands the idea of MGT. Abouelregal et al. [22,23] used the GN-III framework to formulate the heat transfer equation under the influence of a heterogeneous heat source based on the idea of a modified MGT. Marin et al. [24] used the concept of thermoelasticity to examine a dipole fluid under a modified MGT by adding appropriate initial conditions. Using the GN-III [25] thermoelasticity model, the researchers considered thermomechanical waves and plasma waves in the rotating field of a semiconductor. Additionally, using MGT heat transfer theory, Abouelregal et al. [26] examined an endless cylinder-shaped thermoelastic material.

Fractional calculus uses fractional derivatives to study integrals and derivatives of real or complex orders. Fractional calculus has recently gained prominence due to its widespread use in fields as diverse as viscoelasticity, biomedical engineering, and continuum mechanics in physics. It is also widely used in digital signal processing, heat diffusion, bio-biology, dispersion, physical chemistry, and decision theory. Models with genetic decentralization and "long memory" can be quantified using fractional-order differential

equations [27]. Many different formulations describing the concept of fractional derivatives have been proposed and developed [28], and the ideas of derivatives and integrals have been expanded into non-integral orders through different definitions. Major contributors to previous publications are Fourier, Abel, Leibniz, Grünwald, and Letnikov. Liouville and Riemann were two of the most influential mathematicians in the development of the concept of fractional calculus [29].

Photothermal nanomaterials can effectively convert the absorbed solar energy into surface-based local thermal energy. In contrast to conventional photocatalysts that operate at room temperature, photothermal catalysts usually have a much broader solar spectrum and a much higher local reaction temperature. In addition, photothermal catalysis shows the obvious benefits of lower cost and purity using solar energy as a cleaner heat source compared to fossil energy-based thermocatalysis [30]. The foregoing encourages the widespread use of photothermal nanomaterials in various contexts, particularly in environmental and catalytic processes. The application of fractional differential equations has recently attracted much attention as a basis for theoretical models. Because of the memory effect and the fact that it is nonlocal, mathematical frameworks that include a fractional-order differential equation can provide a deeper understanding of the phenomenon. The present work aims to overcome some of the limitations caused by the reliance on physical models of conventional fractional derivatives. Several incorrect-order operators with single and non-unitary kernels have been proposed in the literature [31,32].

Due to the widespread use of photothermal nanomaterials in a variety of fields, especially in environmental and catalytic applications, in the present work, a new, nonlocal anomalous core fractional thermal conduction framework will be proposed to study the behavior of semiconducting solids. To construct the photothermal model, the fractional derivative operator proposed by Atangana–Baleanu–Caputo (ABC) was used in addition to applying the theory of nonlocal contact mechanics. Moreover, the photo-thermoelasticity framework was obtained based on the concept of the Moore–Gibson–Thomson equation [20] and the improvement of Green and Naghdi's third-class theory [17]. To the best of the authors' knowledge, this model is one of the few presented in this context and can be applied to thermoelectric materials with nanostructures and plasmonic structures.

Applying the proposed model, the plasma transfer process and the mechanical thermoelasticity phenomenon are studied in an infinitely flexible semiconductor medium with homogeneous, isotropic, and thermoelastic properties. According to the use of the Laplace transformation and inversion technique, the system of governing equations has been solved, and the analytical solutions have been presented numerically for the domain variables. The effects of thermal parameters, nonlocal factors, and fractional-order index have been shown graphically and tabulated in the Discussion section. In the last section of this paper, the most important conclusions and recommendations that can be drawn from the analysis and study are presented.

2. Mathematical Formulation

In a material that is homogeneous, isotropic, nonlocal, thermoelastic, and semiconducting, the fundamental field equations and the constitutive relations may be stated as [33–38]

$$\tau_{ij}(r) = \int_V \Upsilon\left(|r, r'|, \xi\right)\sigma_{ij}\left(r'\right)\mathrm{d}V\left(r'\right) \tag{1}$$

$$\tau_{ij}(r) - \xi^2\nabla^2\tau_{ij} = \sigma_{ij}\left(r'\right) \tag{2}$$

$$\sigma_{ij} = 2\mu\varepsilon_{ij} + [\lambda\varepsilon_{kk} - \gamma_\theta\theta - \gamma_n N]\delta_{ij}, \tag{3}$$

$$\varepsilon_{ij} = \frac{1}{2}\left(u_{j,i} + u_{i,j}\right) \tag{4}$$

$$\left(1 + \tau_0 D_t^{(\alpha)}\right)\vec{q} = -k\nabla\theta - k^*\nabla\vartheta - \frac{E_g}{\tau}\int N d\vec{r} \tag{5}$$

$$\rho C_e \frac{\partial \theta}{\partial t} + \gamma_\theta T_0 \frac{\partial e}{\partial t} = -\nabla \cdot \vec{q} + Q \tag{6}$$

$$\frac{\partial N}{\partial t} = D_E \nabla^2 N - \frac{N}{\tau} + \kappa\theta \tag{7}$$

$$\tau_{ij,j} + F_i = \rho \frac{\partial^2 u_i}{\partial t^2} \tag{8}$$

In the above equations, the nonlocal stress field is denoted by τ_{ij}, ε_{ij} are the local thermal stress and strain tensors, u_i the displacements, $e = u_{i,i}$, N the phase of carrier intensity, $\theta = T - T_0$ the temperature increment, T_0 the reference temperature, δ_{kl} the Kronecker's delta function, $\gamma_n = (3\lambda + 2\mu)d_n$, $\gamma_\theta = (3\lambda + 2\mu)\alpha_t$, d_n is the electronic deformation parameter, α_t the linear thermal expansion, λ and μ stand for the usual Lame' coefficients, ρ the density, Q external heat sources, k the thermal conductivity, C_e the specific heat, $\vec{q}$ the vector of the heat flux, τ the photo-generated carrier lifetime and E_g the energy gap of the semiconductor, ϑ thermal displacement (satisfies $\dot{\vartheta} = \theta$) and k^* a material constant.

Additionally, $Y(|r, r'|, \xi)$ represents the kernel operator, V the volume, $\xi = e_0 a/l$ is the nonlocal scale coefficient, and a and l are the lengths of the internal and exterior characteristic scales, respectively. The parameter e_0 is an experimentally measured value. The value $e_0 a$ denotes the small-scale parameter.

After inserting Equation (3) into Equation (2), we obtain the nonlocal stress–strain relationships shown below:

$$\tau_{ij} - \xi^2 \nabla^2 \tau_{ij} = 2\mu\varepsilon_{ij} + \lambda\varepsilon_{kk}\delta_{ij} - \gamma_\theta\theta\delta_{ij} - \gamma_n N\delta_{ij} \tag{9}$$

By using Equation (8) in Equation (9), we can obtain:

$$\mu\nabla^2\vec{u} + (\lambda + \mu)\nabla\left(\nabla\cdot\vec{u}\right) - \gamma_\theta\nabla\theta - \gamma_n\nabla N + \left(1 - \xi^2\nabla^2\right)\vec{F} = \rho\left(1 - \xi^2\nabla^2\right)\frac{\partial^2\vec{u}}{\partial t^2} \tag{10}$$

To obtain an improved fractional model for extended thermoelasticity, we replace partial derivatives $\frac{\partial}{\partial t}$ with respect to time t in the revised Fourier law (5) with the fractional differential operator denoted by $D_t^{(\alpha)}$ of order α, $\alpha \in [0,\ 1]$. The symbol $D_t^{(\alpha)}$ means one of the Riemann–Liouville (RL) or Atangana and Baleanu (AB) fractional operators, which are defined by [30,39,40]:

$$\begin{gathered} RLD_t^{(\alpha)}Y(t) = \frac{1}{\Gamma(1-\alpha)}\frac{d}{dt}\int_0^t \frac{Y(\xi)}{(t-\xi)^\alpha}d\xi \\ ABD_t^{(\alpha)}Y(t) = \frac{1}{1-\alpha}\int_0^t E_\alpha\left(-\mu_\alpha(t-\xi)^\alpha\right)\frac{dY(\xi)}{dt}d\xi,\ \mu_\alpha = \frac{\alpha}{1-\alpha},\ \alpha \in [0,\ 1] \end{gathered} \tag{11}$$

The derivative of Equation (5) with respect to the position vector $\vec{r}$ yields

$$\left(1 + \tau_0 D_t^{(\alpha)}\right)\left(\nabla\cdot\vec{q}\right) = -k\nabla^2\theta - k^*\nabla^2\vartheta - \frac{E_g}{\tau}N \tag{12}$$

Once again, by differentiating the above equation with respect to time and utilizing the relationship $\dot{\vartheta} = \theta$, we obtain:

$$\left(1 + \tau_0 D_t^{(\alpha)}\right)\frac{\partial}{\partial t}\left(\nabla\cdot\vec{q}\right) = -\left[k\frac{\partial}{\partial t} + k^*\right]\nabla^2\theta - \frac{E_g}{\tau}\frac{\partial N}{\partial t} \tag{13}$$

After differentiating Equation (6) with respect to time and using Equation (13), we can obtain the fractional Moore–Gibson–Thompson heat transport equation for the semiconductor materials as

$$\left(1 + \tau_0 D_t^{(\alpha)}\right)\left(\rho C_e\frac{\partial^2\theta}{\partial t^2} + T_0\gamma_\theta\frac{\partial^2 e}{\partial t^2} - \frac{\partial Q}{\partial t}\right) - \frac{E_g}{\tau}\frac{\partial N}{\partial t} = \left[k\frac{\partial}{\partial t} + k^*\right]\nabla^2\theta \tag{14}$$

3. Statement of the Problem

The properties of infinite, isotropic, and homogeneous semiconducting media will be studied here. A simplified representation of the proposed case is illustrated in Figure 1. It will be assumed that the studied region $z \geq 0$ is initially quiet and at the reference temperature T_0. It will be assumed that a variable-slope heat source heats the free region above the barrier $z = 0$. The Cartesian coordinates (x, y, z) will be used to study the problem, with the z-axis pointing in a direction perpendicular to the hot surface of the half-space. In this investigation, too, it will be taken into account that all physical fields and temperature changes occur only along the z-axis direction. Thus, the displacement component operates exclusively in the z-axis i.e., $\vec{u} = (0,\ 0,\ w(z,\ t))$.

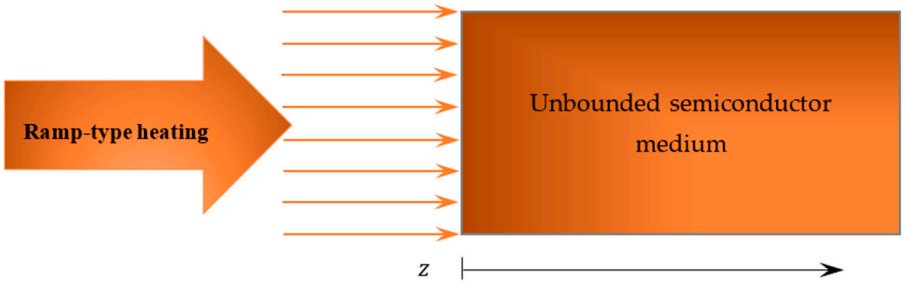

Figure 1. Schematic representation of the thermoelastic semiconductor half-space.

In this illustration, the basic equations can be reconstructed in one dimension in the following manner ($Q = 0$):

$$\rho\left(1-\xi^2\frac{\partial^2}{\partial z^2}\right)\frac{\partial^2 w}{\partial t^2} = (\lambda+2\mu)\frac{\partial^2 w}{\partial z^2} - \gamma_n\frac{\partial N}{\partial z} - \gamma_\theta\frac{\partial \theta}{\partial z} \tag{15}$$

$$\left(1+\tau_0 D_t^{(\alpha)}\right)\left(\rho C_e\frac{\partial^2\theta}{\partial t^2} + \gamma_\theta T_0\frac{\partial^3 w}{\partial z\,\partial t^2}\right) - \frac{E_g}{\tau}\frac{\partial N}{\partial t} = \left[k\frac{\partial}{\partial t} + k^*\right]\frac{\partial^2\theta}{\partial z^2} \tag{16}$$

$$\frac{\partial N}{\partial t} = D_E\frac{\partial^2 N}{\partial z^2} - \frac{N}{t} + k\theta \tag{17}$$

$$\left(1-\xi^2\frac{\partial^2}{\partial z^2}\right)\sigma_{zz} = (\lambda+2\mu)\frac{\partial\, w}{\partial z} - \gamma_n N - \gamma_\theta\theta \tag{18}$$

The following dimensionless variables are defined:

$$\begin{gathered}\{z', w',\ \xi'\} = v_0\eta\{z, w, \xi\}, \{t', \tau_0'\} = v_0^2\eta\{t, \tau_0\}, \sigma_{zz}' = \tfrac{\sigma_{zz}}{\rho v_0^2},\\ \{\theta', N'\} = \tfrac{1}{\rho v_0^2}\{\gamma_\theta\theta, \gamma_n N\}, \eta = \tfrac{\rho C_E}{K}, v_0^2 = \tfrac{\lambda+2\mu}{\rho}.\end{gathered} \tag{19}$$

Basic Equations (15)–(18) can be recast using dimensionless quantities with the primes canceled out as follows:

$$\frac{\partial^2 w}{\partial z^2} - \left(1-\xi^2\frac{\partial^2}{\partial z^2}\right)\frac{\partial^2 w}{\partial t^2} = \frac{\partial}{\partial z}(\theta + N) \tag{20}$$

$$\left(\frac{\partial^2}{\partial z^2} - g_2\frac{\partial}{\partial t} - g_1\right)N = g_3\theta \tag{21}$$

$$\left[\frac{\partial}{\partial t} + \varepsilon_2\right]\frac{\partial^2\theta}{\partial z^2} = \left(1+\tau_0 D_t^{(\alpha)}\right)\left[\frac{\partial^2\theta}{\partial t^2} + \varepsilon_1\frac{\partial^3 w}{\partial z\,\partial t^2} + \varepsilon_3\frac{\partial N}{\partial t}\right] \tag{22}$$

$$\left(1-\xi^2\frac{\partial^2}{\partial z^2}\right)\sigma_{zz} = \frac{\partial\, w}{\partial z} - \theta - N \tag{23}$$

$$g_1 = \frac{\rho}{D_E\eta},\ g_2 = \frac{1}{D_E\eta\tau},\ g_3 = \frac{\kappa d_n}{\gamma\eta^2 D_E v_0^2}, \varepsilon_1 = \frac{\gamma^2 T_0}{\rho^2 C_E v_0^2},\ \varepsilon_2 = \frac{K^*}{v_0^2\eta K}, \varepsilon_3 = \frac{\gamma E_g v_0^2}{\tau d_n K} \tag{24}$$

To arrive at an analytical solution to the suggested problem, it is necessary first to establish the initial conditions listed below:

$$\begin{gathered} w(z,\ t)|_{t=0} = 0 = \left.\frac{\partial w(z,\ t)}{\partial t}\right|_{t=0},\ \ \theta(z,\ t)|_{t=0} = 0 = \left.\frac{\partial \theta(z,\ t)}{\partial t}\right|_{t=0}, \\ N(z,\ t)|_{t=0} = 0 = \left.\frac{\partial N(z,\ t)}{\partial t}\right|_{t=0}. \end{gathered} \tag{25}$$

Using many models, it is possible to gradually raise the temperature controller's active setting to the desired temperature. In order to ensure that the operation strictly adheres to the slope, deviation warnings are frequently used with this function. After maximum incline, the set point enters a "soaking phase," where it remains stationary. The current study examines a thermoelastic homogeneous isotropic stress-free semiconductor medium thermally loaded by ramp-type heating. In this case, we have the following boundary conditions:

$$\theta(z,t) = \begin{cases} 0, & t \le 0 \\ \frac{t_0}{t}, & 0 < t \le t_0 \text{ at } z = 0 \\ 1, & t > t_0 \end{cases} \tag{26}$$

$$\sigma_{zz}(z,t) = 0 \text{ at } z = 0 \tag{27}$$

$$D_E N(z,t) = n_0 \frac{\partial N(z,\ t)}{\partial z} \text{ at } z = 0 \tag{28}$$

where t_0 and n_0 are constants.

Protecting the process from "thermal shock" caused by the controller trying to catch up to a sudden change in the setpoint is what "ramping" means. This is particularly useful in the event of a power outage, as it directs the temperature increase back to the desired level once the electricity is restored.

4. Problem Solution

The Laplace transformation of any function $g(z,\ t)$ can be defined as follows:

$$L(g(z,\ t)) = \overline{g}(z,\ s) = \int_0^\infty g(z,\ t)\exp(-st)dt,\ s > 0 \tag{29}$$

The following results were obtained after Equations (20)–(23) were subjected to a Laplace transform:

$$\left(D^2 - \eta_1\right)\overline{w} = \eta_2 D\overline{\theta} + \eta_2 D\overline{N} \tag{30}$$

$$\left(D^2 - \eta_3\right)\overline{N} = g_3\overline{\theta} \tag{31}$$

$$\left(D^2 - \psi\right)\overline{\theta} = \psi\varepsilon_1 D\overline{w} + \frac{\psi\varepsilon_2}{s}\overline{N} \tag{32}$$

$$\left(1 - \xi^2 D^2\right)\overline{\sigma}_{zz} = D\overline{w} - \overline{\theta} - \overline{N} \tag{33}$$

where

$$\begin{gathered} D = \frac{d}{dz},\ \eta_1 = \frac{s^2}{(1+\xi^2 s^2)},\ \eta_2 = \frac{1}{(1+\xi^2 s^2)}, \\ \eta_3 = (g_1 + g_2 s),\ \psi = \frac{s^2(1+\tau\ \alpha_0)}{s+\varepsilon_2}. \end{gathered} \tag{34}$$

and

$$\alpha_0 = \begin{cases} \text{s}^\alpha \text{ for RL fractional operator,} \\ \frac{s^\alpha}{s^\alpha(1-\alpha)+\alpha} \text{ for AB fractional operator.} \end{cases} \tag{35}$$

By differentiating Equation (30) with regard to z and making use of the connection $\overline{e} = D\overline{w}$, we have found that

$$\left(D^2 - \eta_1\right)\overline{e} = \eta_2 D^2\overline{\theta} + \eta_2 D^2\overline{N} \tag{36}$$

$$\left(D^2 - \psi\right)\overline{\theta} = \psi\varepsilon_1\overline{e} + \frac{\psi\varepsilon_2}{s}\overline{N} \tag{37}$$

$$\left(D^2 - \eta_3\right)\overline{N} = g_3\overline{\theta} \tag{38}$$

Decoupling Equations (36)–(38) yields

$$\left(\mathrm{D}^6 - \delta_1\mathrm{D}^4 + \delta_2\mathrm{D}^2 - \delta_3\right)\left\{\overline{\theta}, \overline{e}, \overline{N}\right\} = 0 \tag{39}$$

where

$$\begin{gathered}\delta_1 = \eta_1 + \eta_8 + \eta_7\eta_5,\ \delta_2 = \eta_1\eta_8 + \eta_7\eta_6 + \eta_9, \delta_3 = \eta_1\eta_9,\\ \eta_5 = \frac{\eta_2}{g_3}, \eta_6 = \frac{\eta_2\eta_3}{g_3} - \eta_2, \eta_7 = \psi g_3\varepsilon_1,\ \eta_8 = \psi + \eta_3,\\ \eta_9 = \frac{g_3\psi\varepsilon_2}{s} + \psi\eta_3.\end{gathered} \tag{40}$$

The following outcomes are achieved when the parameters μ_i, $i = 1, 2, 3$ are inserted in Equation (39):

$$\left(\mathrm{D}^2 - \mu_1^2\right)\left(\mathrm{D}^2 - \mu_2^2\right)\left(\mathrm{D}^2 - \mu_3^2\right)\left\{\overline{\theta}, \overline{e}, \overline{N}\right\} = 0 \tag{41}$$

where the parameters μ_1^2, μ_2^2 and μ_3^2 mean two roots of a given equation:

$$\mu_{\mathrm{i}}^6 - \delta_1\mu_{\mathrm{i}}^4 + \delta_2\mu_{\mathrm{i}}^2 - \delta_3 = 0 \tag{42}$$

The solution to Equation (41) satisfying the radiation requirement that $\overline{\theta}$, $\overline{e}$, and $\overline{N}$ be equal to zero as $z \to \infty$ can be written as follows:

$$\overline{\theta}(z, s) = \sum_{i=1}^{3} A_i e^{-\mu_i z} \tag{43}$$

$$\overline{e}(z, s) = \sum_{i=1}^{3} \Omega_i A_i e^{-\mu_i z} \tag{44}$$

$$\overline{N}(z, s) = -\sum_{i=1}^{3} \Psi_i A_i e^{-\mu_i z} \tag{45}$$

where

$$\Omega_i = \frac{\mu_i^4 - \eta_8\mu_i^2 + \eta_9}{\eta_7},\ \Psi_i = \frac{g_3}{\mu_i^2 - \eta_3}. \tag{46}$$

Additionally, Equations (43)–(45) yield the generic solutions of the field variables $\overline{w}$ and $\overline{\sigma}_{zz}$, which take the following forms:

$$\overline{w}(z, s) = -\sum_{i=1}^{3} \frac{\Omega_i}{\mu_i} A_i e^{-\mu_i z} \tag{47}$$

$$\overline{\sigma}_{zz} = \sum_{i=1}^{3} \Phi_i A_i e^{-\mu_i z} \tag{48}$$

where $\Phi_i = \frac{(\Omega_i - (1 + \Psi_i))}{\left(1 - \xi^2\mu_i^2\right)}$.

The unidentified coefficients A_i, $i = 1, 2, 3$ can be produced by applying various thermal, mechanical, and plasma conditions to the free border of a nonlocal semiconductor medium. We will take into account the ensuing application to calculate it.

As a result of applying the Laplace transformation to the boundary conditions (26)–(28), we obtain:

$$\begin{gathered} \overline{\theta}(0,s) = \frac{1-e^{st_0}}{s^2 t_0} = G(s) \\ \overline{\sigma}_{zz}(0,s) = 0, \\ D_E\, \overline{N}(0,s) = n_0\, D\overline{N}(0,s) \end{gathered} \tag{49}$$

After applying the boundary conditions described above to Equations (43), (45) and (48), we obtain:

$$A_1 + A_2 + A_3 = G(s) \tag{50}$$

$$\Phi_1 A_1 + \Phi_2 A_2 + \Phi_3 A_3 = 0 \tag{51}$$

$$(\Psi_1 - n_0\mu_1)A_1 \ + (\Psi_2 - n_0\mu_2)A_2 \ + (\Psi_3 - n_0\mu_3)A_3 \ = 0 \tag{52}$$

The solution to the previously mentioned set of linear equations gives the values of the unidentified coefficients A_i, where i can take on the values 1, 2, or 3. All the studied fields within the Laplace transform have therefore been completely solved. The Riemann-sum approximation procedure is used to obtain numerical conclusions in the physical domain. The work of Honig and Hirdes [41] provides further details on this strategy.

5. Numerical Results

In the current section, some numerical data will be introduced to study the suggested photo-thermoelasticity model, which was developed to highlight the behavior of temperature, displacement, carrier intensity, and nonlocal thermal stress. The investigation was also conducted by comparing the results of previous work with the results obtained. The values of the following physical coefficients have been taken into consideration, assuming that the material under study is silicon (Si) [42]

$$\lambda = 6.4 \times 10^{10}\left(\frac{\mathrm{N}}{\mathrm{m}^2}\right), \mu = 6.5 \times 10^{10}\left(\frac{\mathrm{N}}{\mathrm{m}^2}\right),$$

$$E_g = 1.11\ eV,\ \rho = 2330\left(\mathrm{kg/m}^3\right), \tau = 5 \times 10^{-10}\ \mathrm{s},$$

$$D_E = 2.5 \times 10^{-3}\left(\mathrm{m}^2/\mathrm{s}\right), d_n = -9 \times 10^{-31}\ \mathrm{m},$$

$$\alpha_t = 4.14 \times 10^{-6}\mathrm{K}^{-1}, C_E = 695\ \mathrm{J/(kg\ K)},$$

$$k = 150\ \mathrm{Wm}^{-1}\mathrm{K}^{-1}, n_0 = 2(\mathrm{m/s}).$$

The Mathematica software package was used to set the numerical computations for all application domains within the medium. The numerical outcomes for the photothermal physical fields are displayed graphically in Figures 1–9 along the z-axis. These graphs and analyses will show how the nonlocal parameter (ξ), thermal relaxation time (τ_0), Atangana and Baleanu differential operators, and fractional order derivatives influence the behavior of the studied field quantities.

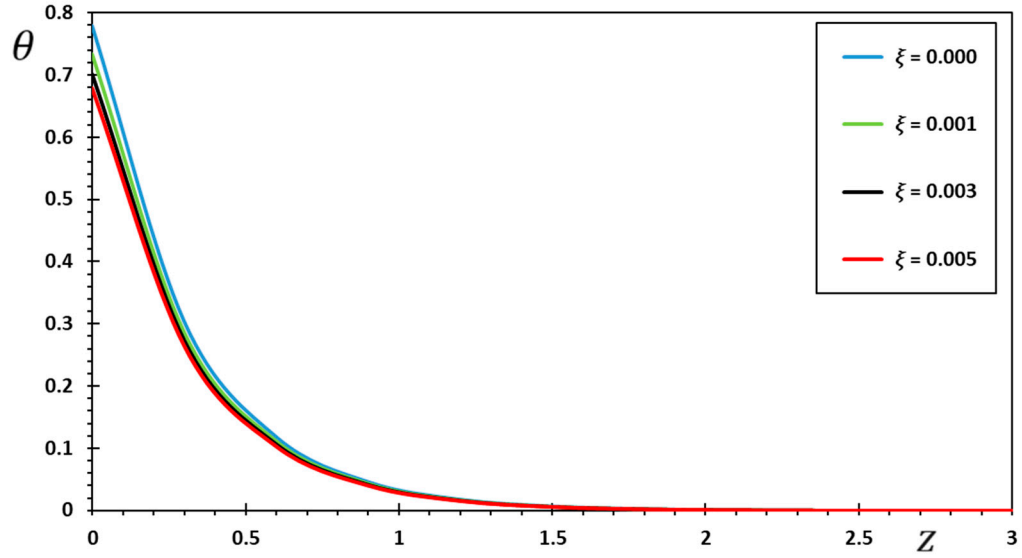

Figure 2. The temperature θ under the influence of small-scale coefficient ξ.

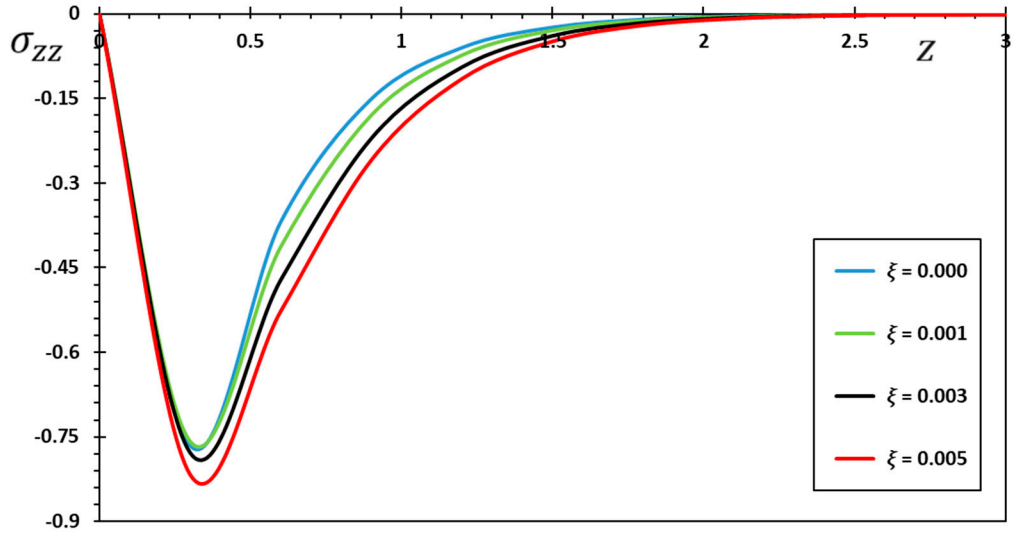

Figure 3. The thermal stress σ_{zz} under the influence of small-scale coefficient ξ.

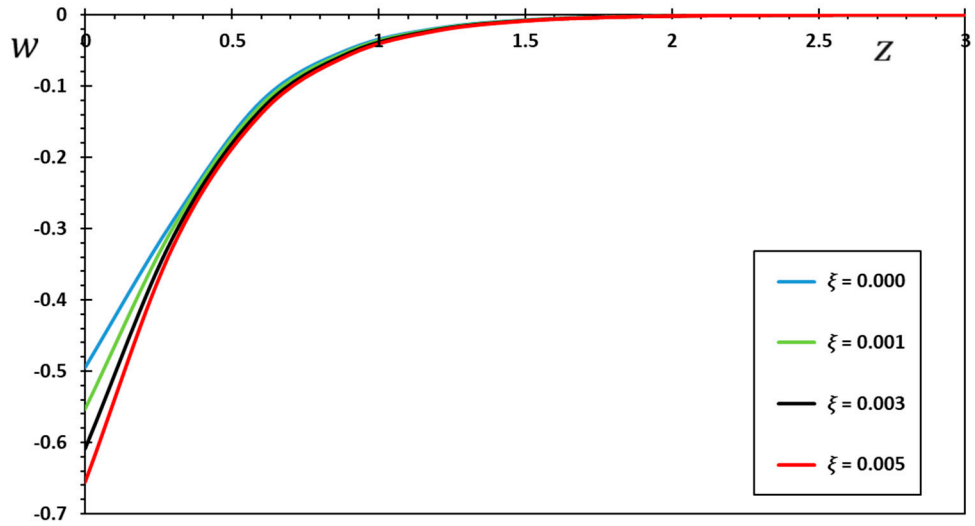

Figure 4. The dimensionless displacement w under the influence of small-scale coefficient ξ.

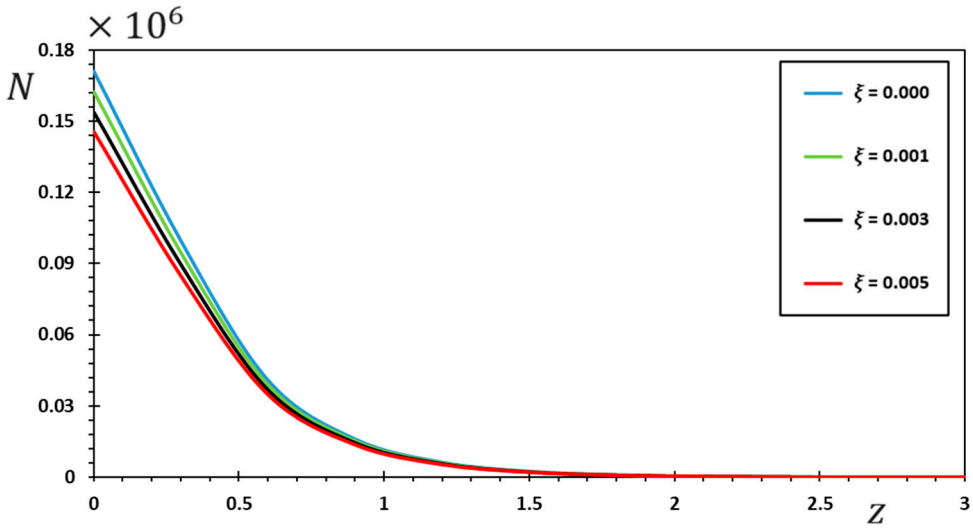

Figure 5. The dimensionless carrier intensity N under the influence of small-scale coefficient ξ.

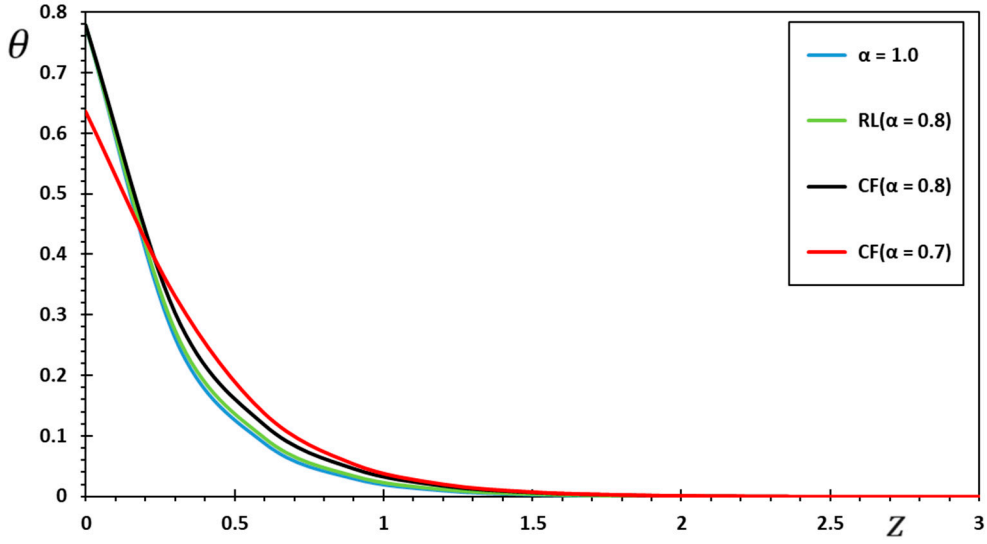

Figure 6. Effect of the AB and RL fractional derivative operators on the dimensionless temperature θ.

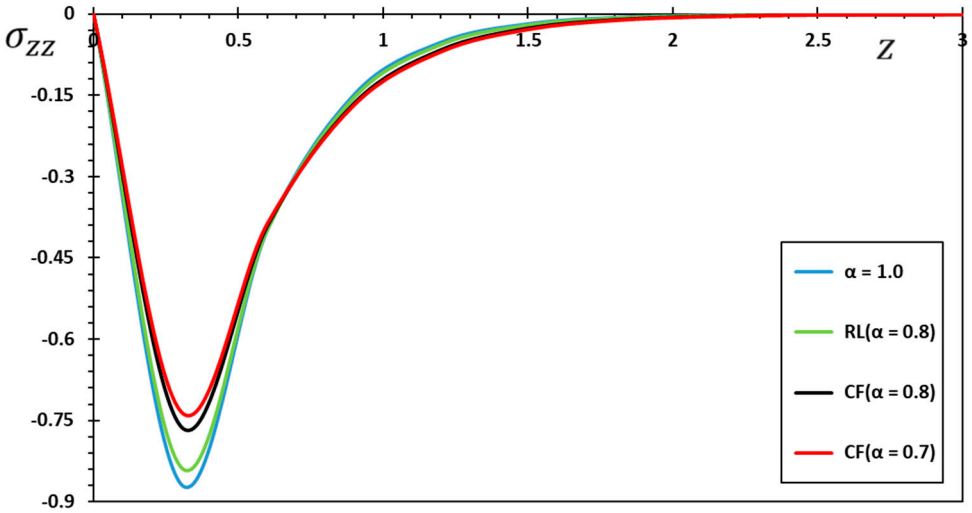

Figure 7. Effect of the AB and RL fractional derivative operators on the nonlocal thermal stress σ_{zz}.

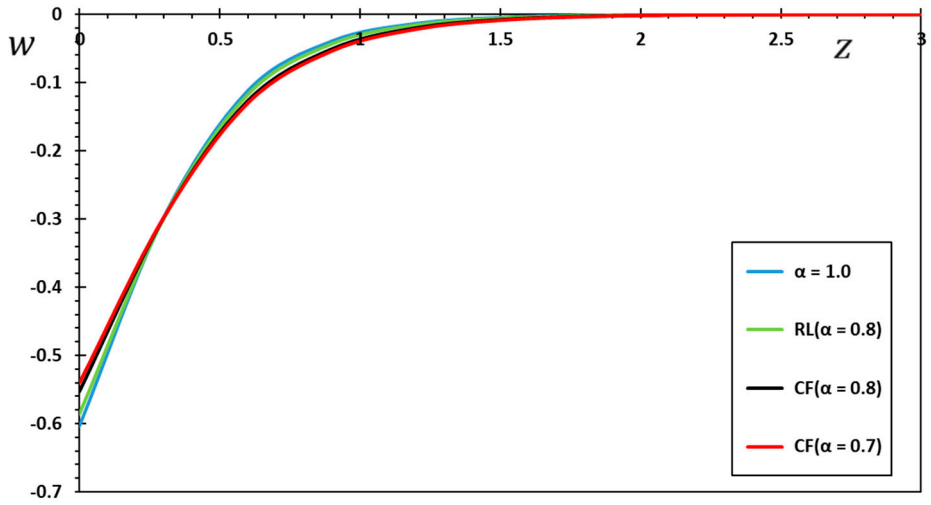

Figure 8. Effect of the CF and RL fractional derivative operators on the dimensionless displacement w.

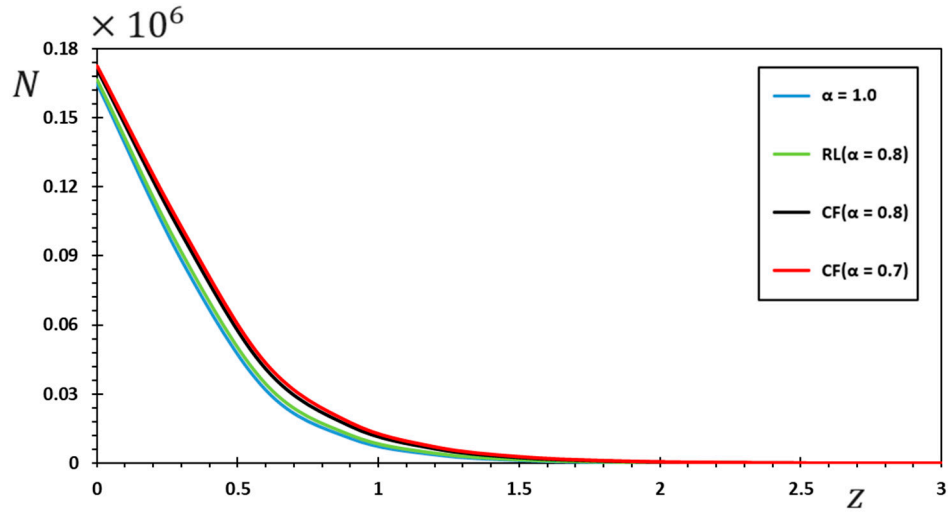

Figure 9. Effect of the AB and RL fractional derivative operators on the carrier intensity N.

5.1. Implications of the Nonlocal Coefficient

In the field of elasticity as well as thermoelasticity, nonlocal concepts have recently received much attention for their multiple applications for modeling small-scale systems. When developing nanoscale devices, the nonlocal continuum theory outperforms the conventional theory compared to alternative methods. However, because many small-scale systems have photothermal properties, there has not been much research on the dynamic response of nanostructured thermoelastic materials. Moreover, fewer computer resources are required to achieve conclusions compared to computationally expensive methodologies such as molecular dynamics simulations.

In this study, the nonlocal Eringen model was used to comprehensively survey the photothermal vibration of an elastic medium in the form of an infinite, nonlocal half-space embedded in a semiconductor material; the effect of macroscopic and microscopic measurements was also considered. To evaluate the impact of the nonlocal modulus on the responses of those semiconducting materials, a numerical discussion of different fields of study such as displacement w, temperature increase, carrier intensity N, and nonlocal thermal stress will be performed. To evaluate the effect of the nonlocal modulus on the responses of these semiconductor materials, different numerical simulations will be

performed for the fields of study. In the calculations, the values of the constants t= 0.12, $\tau_0 = 0.03$, $\alpha = 0.75$, and $t_0 = 0.1$ were taken into account.

It is clear from the graphs that the nonlocal nanoscale coefficient has a significant effect on the spatial diversity of the studied photothermal physical fields. It can be seen that when the nonlocal coefficient is set to zero, the result is the same as in the case of the standard local model of photothermal elasticity. In contrast, in the case of nonlocal models of photothermal elasticity, values $\xi = 0.01$, 0.03, and 0.05 are taken into account.

All these plots show that at $z \to \infty$, all curves converge, and all studied physical domains satisfy the imposed boundary conditions. It is evident from each graph that the values of each thermophysical field are confined to a certain region within the medium near the free surface and do not expand to infinity, which indicates that the speed of propagation of thermal and mechanical waves is limited. These observations are in contrast to the dual photothermal conduction theory, in which the solutions of the system domains tend toward infinity. These findings are consistent with the extended thermoelasticity model concept, which lends credibility to the proposed model and the studied physical facts.

Graph 2 shows the change in temperature θ against distance (z) for different values of the nonlocal coefficient ξ. It can be seen that the maximum temperatures are at the beginning of Figure 2 and then decrease steadily with increasing distance z until they finally stabilize. Further interpretation of the figure reveals that the nonlocality parameter ξ has a clear, though slight, influence on the temperature change θ. The temperature curves decrease with increasing nonlocality parameters ξ. Because of this, researchers have been pushing to formulate theories of modified continuum mechanics that can account for size effects by including intrinsic lengths (see [43] for details).

The nonlocal thermal stress σ_{zz}, shown in Figure 3, varies within a limited region within the semiconducting medium and displays a consistent pattern over a wide range of nonlocal modulus (ξ) values. In Figure 3, it can be noticed that the stress modes σ_{zz} all show zero values initially in accordance with the boundary conditions and then jump to their extreme ranges thereafter before settling back to zero. Outside the perturbation region, the differences disappear, although the nonlocal coefficient (ξ) changes. Moreover, when the value of the nonlocality index increases, the magnitude of the nonlocal thermal stress σ_{zz} increases prominently. This is because the medium is softer with the increase in this nonlocal effect, in accordance with the results of [44]. Raising the length scale indicators has the same impact on both nonlocal models, rising thermal stresses and hence the stiffness of the structure [45].

Along with the distance z and different values of the nonlocality index ξ, the spatial changes of the displacement w are shown in Figure 4. The figure clearly shows that the nonlocal parameter values significantly affect the dynamic displacement field w. It can be seen from the figure that the amount of deformation w within the medium increases with the increase in the values of the nonlocal parameters. When studying an infinite semiconductor material, the nonlocal parameter is a very important part of the thermodynamic deformation of micro/nanostructures.

Like experimental results, displacement (w) values gradually disappear with increasing distance. Thus, the present results showed that the hyperbolic MGT photoelectric heat transfer framework is more accurate from a physical point of view than the Fourier heat transfer model. The reason for this is the limited propagation of mechanical and thermal waves within a semiconductor material because of the relaxation time τ_0.

Hyperbolic heat transfer has recently been verified experimentally in heterogeneous materials such as sand and NaHCO3, with a relaxation time of approximately 20 s [46], in supercooled materials such as graphite [47], and biological materials such as lipid films [48]. The delay in the interaction between convection flux and temperature gradient, caused by the heterogeneous structures, appears to be the mechanism by which waves are induced. The phase lag may indicate the time required for sufficient heat to build up to cause large convection currents to flow between structural parts [46]. This behavior of a heat wave is

not predicted by the classical Fourier law, which allows heat flow to respond quickly to changes in the temperature gradient [49].

The graph in Figure 5 depicts the relationship between carrier intensity N and nonlocality ξ as depth z changes. Except for the magnitude, the behavior of the carrier density N is very consistent across all the different cases. With nonlocality ξ decreasing, the effect of the nonlocality index on the carrier density profile over time appears to be weak. As the nonlocal parameter ξ increases, the magnitude of the carrier density, N, decreases.

As a result of the high thermal load from ramp-type heating, a nonlocal index is required for both static and dynamic studies of a micro- or nanoscale semiconductor medium. It is the value of the nonlocal parameter that determines when the waves will reach the steady state, as seen in Figures 2–5. These results, along with the preceding explanation, show that the microscale impact is not detectable in structures with dimensions on the nanometer scale. At the same time, it may be seen in nanostructures, as corroborated by the results found by Abouelregal [50] and Cong and Duc [51]. Moreover, the nonlocal responses are an essential factor that cannot be ignored when trying to estimate the stress at the origin of a nanoscale thermal problem [52]. While the Fourier model predicts that heat will spread instantly across a sample, the tests were meant to demonstrate that it really takes a finite amount of time (relaxation time τ_0) for heat waves to reach a specific place inside the sample [53].

5.2. The Influence of the Fractional Operators

The rapid emergence of fractional calculus has attracted many researchers in many different applied fields. Based on many theoretical and experimental studies, it was found that physical systems with fractal order are superior to the traditional ones that include integer orders. Not only that, but it also turns out to be more of a reflection of reality. As in the present work, many real properties of semiconductor nanostructures can be represented more accurately by proposing nonlocal photothermal models that incorporate the fractional-order derivative.

In this sub-section of the discussion, the effects of ramp-type heating on a nonlocal half-area of a thermal semiconductor will be explored with a change in the fractional operator as well as the fractional order. The numerical results for all studied physical fields were calculated when values of $\xi = 0.01$, $\tau_0 = 0.02$ and $t_0 = 0.1$ were taken into account. The numerical results are represented graphically in Figures 6–9 during the range $0 \leq z \leq 3$. We will set the value $\alpha = 1$ in the context of the nonlocal extended theory of MGT thermo-optical elasticity with one phase delay and no fractional actuators. When $0 < \alpha < 1$, the numerical results will be compared in the case of the nonlocal MGT photothermoelasticity model, which includes fractional actuators with both the Atangana and the Baleanu (AB) operator or Riemann–Liouville (RL) fractional operator. For each of the fractional operators, two different values of the fractional order will be taken ($\alpha = 0.8$ and $\alpha = 0.7$).

It is clear that the effects of the fractional order coefficient α and the nonlocal fractional differential operators proposed by Atangana and Baleanu (AB) are striking. It is evident that the curves and behavior of the studied fields change according to the operator used, as well as the order of the fractional differential (α). We suggest that time-dependent fractional differentiation may be understood as the presence of memory effects that match the system's inherent dissipation. Sheikh et al. [54] discussed some of the characteristics of this new phenomenon, and there was some agreement on the same behavior.

In addition, thermomechanical waves reach a steady state depending on the selected fractal order (α) values. An important observation that must be taken into account is the superiority of the improved fractional operator AB over the traditional fractional operator (RL) in terms of memory effect. It is noted that the amplitude values of the different fields studied in the case of the fractional operator AB are less than in the case of using the conventional operator (RL). In addition, using higher-order values of fractal differential improves the process of thermal conductivity as it slows down the speed of heat waves, which is assumed to be infinite in the case of the conventional model of thermoelasticity.

For different values of the chemical reaction model in [55], similar behavior can be seen in terms of speed and temperature.

Looking at all Figure 7, it is clear that the nonlocal thermal stress σ_{zz} that are being examined move away from the free surface of the material that is affected by the changing thermal field, and the waves dissipate faster within the medium. Thermal stress is compressive as a result of deformation due to thermal loading. One of the most significant observations from these results is the inverse proportion of fractional modulus (α) values to wave propagation, as it was shown that they fade faster with increasing fractional modulus values. Thus, it can be said that when the value of the fractional parameter (α) grows, the temperature change θ, displacement u, and carrier force N all grow, but in the case of nonlocal thermal stress σ_{xx}, they decrease. The findings also suggest that the Atangana–Baleanu fractional concept is more rapid than the Riemann–Liouville fractional version for calculating fractional derivatives. The results observed by Khan et al. [56] are strongly consistent with the study conducted. All of this demonstrates the reliability of the suggested model and the importance of the present effort.

The Atangana and Baleanu (AB) fractional derivatives provide a more realistic representation of the world than the one that makes use of a power function kernel [57]. This is due to the fact that the singularity does not take place at the end of the interval that is used to calculate the fractional derivative of a function. This occurrence corresponds to the description that is given in [58]. The power function is a worse filter than the exponent function, so the best choice is the fractional derivative, whose kernel is the exponent function. In fact, the Atangana and Baleanu fractional derivative has seen quite a bit of activity in the realm of filter control [30].

The figures also show that the behavior of the fields in the nonlocal differential operator of Atangana and Baleanu (AB) is less than in the case of the Riemann–Liouville (RL) operator. Finally, it is worth mentioning that this new fractional derivative operator (Atangana and Baleanu (AB)) will play a pivotal role in the investigation of the macroscopic behavior of semiconductor materials where nonlocal interactions play a potential role in determining the properties of materials [59]. Thermoelastic models, including fractional derivatives of non-integer orders, are effective for explaining heat transfer processes and semiconductor systems with exponentially distributed delays.

6. Conclusions

This study develops a new nonlocal photo-thermoelasticity model to describe the coupling between plasma and thermomechanical waves in semiconductors. Nonlocal elasticity theory and the concept of extended MGT thermal conductivity with time derivatives with fractional operators are both included in the proposed framework. To solve some problems of traditional fractional models, the fractional derivative proposed by Atangana and Baleanu (AB) (described by Mittag–Leffler functions), which includes a non-singular and nonlocal kernel, has been taken into account. The governing differential equations are solved using Laplace transforms. System parameter simulations of silicon as a semiconductor material were presented and analyzed using graphical representations of the data. The following are the most important conclusions that can be drawn from the discussion and analysis:

- Nonlocal factors have a significant role in changing the behavior of thermomechanical interactions in small-sized semiconductor materials. As a result, when modeling nonlocal microstructures, the value of the nonlocal coefficient must be chosen very carefully.
- The new nonlocal photothermal model predicts smaller amounts than those in the case of the traditional (local) photothermal model. For this reason, nanoscale factors must be included in reducing the mechanical wave behavior of (nonlocal) nanostructures.
- The fractional-order index can be used to reclassify semiconductor materials in terms of photoelectric thermal conductivity. The fractional coefficient of the derivative operator of Atangana and Baleanu slightly affects the rate of temperature fluctuation. Thermoplastic models with fractional derivatives have much larger standard devi-

ations than thermoplastic models. As a result, the fractional coefficient is gaining ground as an excellent thermal indicator.

- When using fractional actuators, the values of the thermo-photophysical fields were found to be lower compared to what would be expected by conventional thermophotometric models. Therefore, by varying the fractional parameter, we may be able to estimate the function that the Atangana and Baleanu derivative operators play in heat transfer regimes and perform more detailed examinations of elastic thermal deformation in rigid mechanics. The method and results from this work can also be used to solve similar problems in thermoelasticity and thermodynamics.

Author Contributions: Conceptualization, A.E.A. and S.A.; methodology, M.M.; software, S.A.; validation, A.E.A., A.F. and M.M.; formal analysis, M.M.; investigation, A.F.; resources, A.E.A.; data curation, S.A. and A.F.; writing—original draft preparation, A.E.A. and M.M.; writing—review and editing, S.A.; visualization, A.F.; supervision, M.M.; project administration, A.E.A.; funding acquisition, A.E.A. All authors have read and agreed to the published version of the manuscript.

Funding: This work was supported by Deputyship for Research & Innovation, Ministry of Education in Saudi Arabia IFKSURG-1228.

Data Availability Statement: Not applicable.

Acknowledgments: The authors extend their appreciation to the Deputyship for Research & Innovation, Ministry of Education in Saudi Arabia for funding this research work through the project no. (IFKSURG-1228).

Conflicts of Interest: The authors declared no potential conflict of interest with respect to the research, authorship, and publication of this article.

References

1. Gärtner, W.W. Photothermal Effect in Semiconductors. *Phys. Rev.* **1961**, *122*, 419. [CrossRef]
2. Jin, H.; Lin, G.; Bai, L.; Zeiny, A.; Wen, D. Steam generation in a nanoparticle-based solar receiver. *Nano Energy* **2016**, *28*, 397–406. [CrossRef]
3. Liu, F.; Lai, Y.; Zhao, B.; Bradley, R.; Wu, W. Photothermal materials for efficient solar powered steam generation. *Front. Chem. Sci. Eng.* **2019**, *13*, 636–653. [CrossRef]
4. Abbas, I.; Hobiny, A.D. Analytical-numerical solutions of photothermal interactions in semiconductor materials. *Inf. Sci. Lett.* **2021**, *10*, 189.
5. Todorovic, D.M.; Galović, S.; Popovic, M. Optically excited plasmaelastic waves in semiconductor plate-coupled plasma and elastic phenomena. *J. Phys. Conf. Ser.* **2010**, *214*, 012106. [CrossRef]
6. Vasil'ev, A.N.; Sablikov, V.A.; Sandomirskii, V.B. Photothermal and photoacoustic effects in semiconductors and semi-conductor structures. *Soviet Phys. J.* **1987**, *30*, 544–554. [CrossRef]
7. Abouelregal, A.E.; Sedighi, H.M.; Sofiyev, A.H. Modeling photoexcited carrier interactions in a solid sphere of a sem-iconductor material based on the photothermal Moore–Gibson–Thompson model. *Appl. Phys. A* **2021**, *127*, 845. [CrossRef]
8. Pradhan, S.C.; Murmu, T. Small scale effect on the buckling of single-layered graphene sheets under biaxial com-pression via nonlocal continuum mechanics. *Comput. Mater. Sci.* **2009**, *47*, 268–274. [CrossRef]
9. Wang, C.Y.; Murmu, T.; Adhikari, S. Mechanisms of nonlocal effect on the vibration of nanoplates. *Appl. Phys. Lett.* **2011**, *98*, 153101. [CrossRef]
10. Eringen, A. Theory of nonlocal thermoelasticity. *Int. J. Eng. Sci.* **1974**, *12*, 1063–1077. [CrossRef]
11. Eringen, A.C. On differential equations of nonlocal elasticity and solutions of screw dislocation and surface waves. *J. Appl. Phys.* **1983**, *54*, 4703–4710. [CrossRef]
12. Eringen, A.C.; Edelen, D.G.B. On nonlocal elasticity. *Int. J. Eng. Sci.* **1972**, *10*, 233–248. [CrossRef]
13. Eringen, A.; Wegner, J. Nonlocal Continuum Field Theories. *Appl. Mech. Rev.* **2003**, *56*, B20–B22. [CrossRef]
14. Biot, M.A. Thermoelasticity and Irreversible Thermodynamics. *J. Appl. Phys.* **1956**, *27*, 240–253. [CrossRef]
15. Lord, H.; Shulman, Y. A generalized dynamical theory of thermoelasticity. *J. Mech. Phys. Solids* **1967**, *15*, 299–309. [CrossRef]
16. Green, A.E.; Naghdi, P.M. A re-examination of the basic postulates of thermomechanics. *Proc. R. Soc. London Ser. A Math. Phys. Sci.* **1991**, *432*, 171–194. [CrossRef]
17. Green, A.E.; Naghdi, P.M. ON UNDAMPED HEAT WAVES IN AN ELASTIC SOLID. *J. Therm. Stress.* **1992**, *15*, 253–264. [CrossRef]
18. Green, A.E.; Naghdi, P.M. Thermoelasticity without energy dissipation. *J. Elast.* **1993**, *31*, 189–208. [CrossRef]
19. Lasiecka, I.; Wang, X. Moore–Gibson–Thompson equation with memory, part II: General decay of energy. *J. Diff. Eqns.* **2015**, *259*, 7610–7635. [CrossRef]
20. Quintanilla, R. Moore-Gibson-Thompson thermoelasticity. *Math. Mech. Solids* **2019**, *24*, 4020–4031. [CrossRef]

21. Quintanilla, R. Moore-Gibson-Thompson thermoelasticity with two temperatures. *Appl. Eng. Sci.* **2020**, *1*, 100006. [CrossRef]
22. Abouelregal, A.; Ahmed, I.-E.; Nasr, M.; Khalil, K.; Zakria, A.; Mohammed, F. Thermoelastic Processes by a Continuous Heat Source Line in an Infinite Solid via Moore–Gibson–Thompson Thermoelasticity. *Materials* **2020**, *13*, 4463. [CrossRef] [PubMed]
23. Abouelregal, A.E.; Marin, M. The response of nanobeams with temperature-dependent properties using state-space method via modified couple stress theory. *Symmetry* **2020**, *12*, 1276. [CrossRef]
24. Marin, M.; Öchsner, A.; Bhatti, M.M. Some results in Moore-Gibson-Thompson thermoelasticity of dipolar bodies. *J. Appl. Math. Mech.* **2020**, *100*, e202000090. [CrossRef]
25. Abouelregal, A.E.; Marin, M.; Askar, S. Thermo-Optical Mechanical Waves in a Rotating Solid Semiconductor Sphere Using the Improved Green–Naghdi III Model. *Mathematics* **2021**, *9*, 2902. [CrossRef]
26. Abouelregal, A.; Ersoy, H.; Civalek, Ö. Solution of Moore–Gibson–Thompson Equation of an Unbounded Medium with a Cylindrical Hole. *Mathematics* **2021**, *9*, 1536. [CrossRef]
27. Podlubny, I.; Chechkin, A.; Skovranek, T.; Chen, Y.; Jara, B.M.V. Matrix approach to discrete fractional calculus II: Partial fractional differential equations. *J. Comput. Phys.* **2009**, *228*, 3137–3153. [CrossRef]
28. Hobiny, A.; Abbas, I. The Effect of a Nonlocal Thermoelastic Model on a Thermoelastic Material under Fractional Time Derivatives. *Fractal Fract.* **2022**, *6*, 639. [CrossRef]
29. Podlubny, I. *Fractional Differential Equations: An Introduction to Fractional Derivatives, Fractional Differential Equa-tions, to Methods of Their Solution and Some of Their Applications*; Elsevier: Amsterdam, The Netherlands, 1998; Volume 198.
30. Wu, X.; Chen, G.Y.; Owens, G.; Chu, D.; Xu, H. Photothermal materials: A key platform enabling highly efficient water evaporation driven by solar energy. *Mater. Today Energy* **2019**, *12*, 277–296. [CrossRef]
31. Atangana, A.; Baleanu, D. New fractional derivatives with nonlocal and non-singular kernel: Theory and application to heat transfer model. *Therm. Sci.* **2016**, *20*, 763–769. [CrossRef]
32. Caputo, M.; Fabrizio, M. A new definition of fractional derivative without singular kernel. *Prog. Fract. Differ. Appl.* **2015**, *1*, 73–85.
33. Bachher, M.; Sarkar, N. Nonlocal theory of thermoelastic materials with voids and fractional derivative heat transfer. *Waves Random Complex Media* **2019**, *29*, 595–613. [CrossRef]
34. Ebrahimi, F.; Haghi, P. Elastic wave dispersion modelling within rotating functionally graded nanobeams in thermal environment. *Adv. Nano Res.* **2018**, *6*, 201–217.
35. Kaur, I.; Singh, K. Plane wave in non-local semiconducting rotating media with Hall effect and three-phase lag fractional order heat transfer. *Int. J. Mech. Mater. Eng.* **2021**, *16*, 14. [CrossRef]
36. Zhou, H.; Shao, D.; Song, X.; Li, P. Three-dimensional thermoelastic damping models for rectangular micro/nanoplate resonators with nonlocal-single-phase-lagging effect of heat conduction. *Int. J. Heat Mass Transf.* **2022**, *196*, 123271. [CrossRef]
37. Todorović, D.M. Plasma, thermal, and elastic waves in semiconductors. *Rev. Sci. Instrum.* **2003**, *74*, 582–585. [CrossRef]
38. Song, Y.Q.; Bai, J.T.; Ren, Z.Y. Study on the reflection of photothermal waves in a semiconducting medium under gen-eralized thermoelastic theory. *Acta Mech.* **2012**, *223*, 1545–1557. [CrossRef]
39. Nonnenmacher, T.F.; Metzler, R. On the Riemann-Liouville Fractional Calculus and Some Recent Applications. *Fractals* **1995**, *3*, 557–566. [CrossRef]
40. Wang, J.; Ye, Y.; Pan, X.; Gao, X.; Zhuang, C. Fractional zero-phase filtering based on the Riemann–Liouville integral. *Signal Process.* **2014**, *98*, 150–157. [CrossRef]
41. Honig, G.; Hirdes, U. A method for the numerical inversion of Laplace transforms. *J. Comput. Appl. Math.* **1984**, *10*, 113–132. [CrossRef]
42. Abouelregal, A.E.; Sedighi, H.M.; Shirazi, A.H. The Effect of Excess Carrier on a Semiconducting Semi-Infinite Medium Subject to a Normal Force by Means of Green and Naghdi Approach. *Silicon* **2021**, *14*, 4955–4967. [CrossRef]
43. Sumelka, W.; Zaera, R.; Fernández-Sáez, J. A theoretical analysis of the free axial vibration of nonlocal rods with frac-tional continuum mechanics. *Meccanica* **2015**, *50*, 2309–2323. [CrossRef]
44. Karličić, D.; Kozić, P.; Pavlović, R. Free transverse vibration of nonlocal viscoelastic orthotropic multi-nanoplate system (MNPS) embedded in a viscoelastic medium. *Compos. Struct.* **2014**, *115*, 89–99. [CrossRef]
45. Aydogdu, M. Axial vibration of the nanorods with the nonlocal continuum rod model. *Phys. E Low-Dimens. Syst. Nanostructures* **2009**, *41*, 861–864. [CrossRef]
46. Kaminski, W. Hyperbolic heat conduction for materials with a non-homogeneous inner structure. *ASME J. Heat Transf.* **1990**, *112*, 555–560. [CrossRef]
47. Wall, D.J.N.; Olsson, P. Invariant imbedding and hyperbolic heat waves. *J. Math. Phys.* **1997**, *38*, 1723–1749. [CrossRef]
48. Mitra, K.; Kumar, S.; Vedevarz, A.; Moallemi, M.K. Experimental Evidence of Hyperbolic Heat Conduction in Processed Meat. *J. Heat Transf.* **1995**, *117*, 568–573. [CrossRef]
49. Abdel-Hamid, B. Modelling non-Fourier heat conduction with periodic thermal oscillation using the finite integral transform. *Appl. Math. Model.* **1999**, *23*, 899–914. [CrossRef]
50. Abouelregal, A.E. A novel model of nonlocal thermoelasticity with time derivatives of higher order. *Math. Methods Appl. Sci.* **2020**, *43*, 6746–6760. [CrossRef]
51. Cong, P.H.; Duc, N.D. Effect of nonlocal parameters and Kerr foundation on nonlinear static and dynamic stability of micro/nano plate with graphene platelet reinforcement. *Thin-Walled Struct.* **2023**, *182*, 110146. [CrossRef]

52. Numanoğlu, H.M.; Ersoy, H.; Akgöz, B.; Civalek, Ö. A new eigenvalue problem solver for thermo-mechanical vibration of Timoshenko nanobeams by an innovative nonlocal finite element method. *Math. Methods Appl. Sci.* **2021**, *45*, 2592–2614. [CrossRef]
53. Herwig, H.; Beckert, K. Fourier Versus Non-Fourier Heat Conduction in Materials with a Nonhomogeneous Inner Structure. *J. Heat Transf.* **1999**, *122*, 363–365. [CrossRef]
54. Sheikh, N.A.; Ali, F.; Saqib, M.; Khan, I.; Alam Jan, S.A.; Alshomrani, A.S.; Alghamdi, M.S. Comparison and analysis of the Atangana–Baleanu and Caputo–Fabrizio fractional derivatives for generalized Casson fluid model with heat generation and chemical reaction. *Results Phys.* **2017**, *7*, 789–800. [CrossRef]
55. Ali, F.; Alam Jan, S.A.; Khan, I.; Gohar, M.; Sheikh, N.A. Solutions with special functions for time fractional free convection flow of Brinkman-type fluid. *Eur. Phys. J. Plus* **2016**, *131*, 310. [CrossRef]
56. Khan, A.; Abro, K.A.; Tassaddiq, A.; Khan, I. Atangana–Baleanu and Caputo Fabrizio Analysis of Fractional Derivatives for Heat and Mass Transfer of Second Grade Fluids over a Vertical Plate: A Comparative Study. *Entropy* **2017**, *19*, 279. [CrossRef]
57. Xu, H.; Zhang, L.; Wang, G. Some New Inequalities and Extremal Solutions of a Caputo–Fabrizio Fractional Bagley–Torvik Differential Equation. *Fractal Fract.* **2022**, *6*, 488. [CrossRef]
58. Alqahtani, R.T. Fixed-point theorem for Caputo–Fabrizio fractional Nagumo equation with nonlinear diffusion and convection. *J. Nonlinear Sci. Appl.* **2016**, *9*, 1991–1999. [CrossRef]
59. Goufo, E.F.D. Application of the Caputo-Fabrizio fractional derivative without singular kernel to Korteweg-de Vries-Bergers equation. *Math. Model. Anal.* **2016**, *21*, 188–198. [CrossRef]